STUDY ON TEMPERATURE MEASUREMENT AND EXPERIMENT OF LOOSE COAL BASED ON ACOUSTIC THERMOMETRY

Yuxin YE, Peizhe ZOU, Chao HAN, Xiaoyu LIANG *

College of Energy Environment and Safety Engineering, China Jiliang University, Hangzhou 310018, China

* Corresponding author, E-mail address: xyliang@cjlu.edu.cn

In order to enhance the accuracy of temperature measurement for loose coal using acoustic methods, this study constructed an experimental system based on the principle of acoustic thermometry. The system was designed to investigate the influence mechanisms of acoustic signal frequency, sensor spacing and temperature on the acoustic wave propagation characteristics. The acoustic wave transit time was measured under different frequency ranges, sensor spacings, and temperature conditions during the experiments. The results show that the acoustic transit time tends to stabilize in the range of 400-1000 Hz and 2000-3000 Hz, and the acoustic wave propagation effect is superior, which is more suitable for the preferred frequency range of the acoustic wave transit time test. The acoustic wave transit time increases with the sensor spacing, and the growth rate of the acoustic transit time in different frequency ranges shows a significant difference. As temperature rises, the acoustic wave transit time shows a decreasing trend, and the relative error between the inverted temperature and the reference temperature based on the acoustic temperature measurement model is 2.27%-7.13%, which verifies the reliability and accuracy of the model. This study provides important theoretical foundations and experimental basis for the accurate measurement of spontaneous combustion temperature in loose coal.

Keywords: *Acoustic temperature measurement, Loose coal, Coal spontaneous combustion, Acoustic wave transit time*

1.Introduction

China's primary energy presents the characteristics of "rich in coal, lack of oil, less gas", and according to the latest China Mineral Resources Report released by the Ministry of Natural Resources, China's coal consumption accounts for 55.3% of the total primary energy consumption [1]. This indicates that China's coal-based energy structure is difficult to change in the short term, and coal remains the primary energy source in China [2]. During production, transportation and storage, stacked coal is easily forms heat accumulation zones, increasing the risk of spontaneous combustion [3, 4]. Studies show that spontaneous combustion in stacked coal is hidden, slow, and complex. Traditional methods have difficulty measuring internal temperature and heat transfer. In early stages, there are no clear external signs, making early detection and prevention particularly challenging [5, 6].

Acoustic temperature measurement technology has attracted much attention in recent years for

its wide range, excellent spatial flexibility, real-time monitoring and non-contact capabilities. It has been effectively applied in utility boilers, lakes, atmosphere, stored biomass and grain [7-11]. Kong et al. [12] employed acoustic wave propagation characteristics to analyze their interaction with temperature and velocity fields, enabling accurate measurement of boiler temperature distribution. Yan et al. [13] proposed a passive acoustic method using a Fabry-Perot resonator (AFPR) and demonstrated its effectiveness for monitoring atmospheric boundary layer temperature by linking resonance frequency to mode order. Huang et al. [14] extracted and evaluated three multipath signals to confirm the reliability and efficiency of Coastal Acoustic Tomography (CAT) for continuous temperature monitoring in small lakes. Yan et al. [15, 16] developed an acoustic tomography technique for monitoring grain temperature. They established a model linking temperature and acoustic time difference and introduced a velocity correction factor, confirming the feasibility of acoustic thermometry within bulk grain for the first time.

In acoustic temperature measurement of loose coal, Guo et al.[17-19] proposed the concept of dual-source composite acoustic wave, introducing pseudo-random sequences as excitation signals. By combining these with a quadratic correlation PHAT-β algorithm, they optimized signal processing and achieved high-precision transit time measurements (error < 5%). Wang et al.[20] combined acoustic temperature sensing with gas analysis and observed abrupt changes in transit time during O_2 drops. Lower coal metamorphism led to faster sound speeds and higher combustion risk. They developed a risk grading and early warning system integrating both data types to improve monitoring accuracy and response. Deng et al.[21] compared excitation signals and identified linear swept signals as the most suitable due to low temperature sensitivity and minimal low-frequency attenuation. Kong et al.[22] used the SIRT algorithm to reconstruct the wave velocity field, revealing that high-velocity regions corresponded to high-temperature zones, effectively tracking temperature changes during heating.

Building on previous research, this study focuses on practical experimental conditions for acoustic temperature measurement in loose coal. The effects of sensor spacing on acoustic wave stability and signal attenuation were evaluated, and a characteristic factor (λ) was introduced to correct acoustic transit time, enhancing the comparability and adaptability of temperature inversion under various frequency-spacing combinations. An acoustic measurement system was developed and tested across a frequency range of 200-3000 Hz, sensor spacings of 0.15-0.75 m, and temperatures of 20-50 °C. The acoustic transit time variations were systematically analyzed to reveal the coupled influence of frequency, spacing, and temperature on wave propagation, providing a basis for developing an accurate acoustic temperature model.

2.Principles of acoustic temperature measurement

According to the acoustic wave equation in an ideal fluid coal mass, the relationship between the propagation velocity of sound waves and the pressure and density is as follows [23]:

$$c^2 = \frac{dP}{d\rho} \tag{1}$$

The adiabatic process equation for ideal gas (also known as Poisson's equation) is as follows:

$$PV^{\gamma} = const \tag{2}$$

where: V is the volume of the ideal gas, γ is the specific heat capacity ratio.

Assuming that the ideal gas mass is constant, the above equation can be further derived as:

$$\frac{P}{\rho^{\gamma}} = const \tag{3}$$

Substituting eq. (1) into eq. (3) gives:

$$c^2 = \frac{\gamma P}{\rho} \tag{4}$$

The ideal gas equation of state is given by:

$$PV = \frac{M}{\mu} RT \tag{5}$$

where: M is gas mass, μ is the molar amount of gas, the molar amount of air is 29×10^{-3} kg/mol, R is the gas constant, R=8.31 kJ/(K·mol).

According to eq (5) the velocity of sound waves can be expressed as:

$$c = \sqrt{\frac{\gamma R}{\mu} T} = Z\sqrt{T} \tag{6}$$

Since γ, R and μ are known quantities in air, Z is defined as the velocity of sound constant of the gaseous medium, the value of Z is calculated to be 20.045.

This gives the temperature in free space as:

$$T = \left(\frac{c}{Z}\right)^2 \tag{7}$$

A loudspeaker and two acoustic sensors are installed in the measured area. When the path, distance l, and acoustic wave transit time t are known, the sound velocity in free space is:

$$c = \frac{l}{t} \tag{8}$$

Acoustic wave propagation in loose coal is influenced by frequency and porosity, affecting both attenuation and velocity. Increased porosity promotes gas diffusion and adsorption [24], causing velocity variations under different pore structures and physical conditions. To improve accuracy and ensure measurement consistency, a characteristic factor λ was introduced [17].

Further derivation gives the average temperature of the path as:

$$T = \left(\frac{\lambda l}{tZ}\right)^2 \tag{9}$$

In summary, the key parameters of the acoustic temperature measurement technique comprise sensor spacing, acoustic wave transit time and the sound velocity constant of the gas medium. Since sound velocity in the gas medium and sensor spacing are known, the average temperature along that path can be calculated by accurately measuring the acoustic wave transit time along a path.

3.Acoustic wave transit time calculation

According to the cross-correlation algorithm, the signal crossing time can be obtained by calculating the correlation degree between two signals [25]. The function is calculated at different delay points, and the transit time corresponds to the delay with the maximum correlation value [26].

Assuming that $x_1(t)$ and $x_2(t)$ are the signals received by a pair of acoustic sensors, and $s(t)$ are the sound source signals, then the two signals can be represented as:

$$\begin{aligned} x_1(t) &= s(t) + n_1(t) \\ x_2(t) &= \alpha s(t - D) + n_2(t) \end{aligned} \tag{10}$$

where: α is the attenuation coefficient of the acoustic wave amplitude, $n_1(t)$ and $n_2(t)$ are the noise of the signal. D is the actual acoustic wave transit time from acoustic sensor 1 to sensor 2.

The cross-correlation function of $x_1(t)$ and $x_1(t)$ can be expressed as:

$$R_{x_1x_2}(\tau) = \alpha \int_{+\infty}^{-\infty} x_1(t) + x_2(t-\tau)d\tau \tag{11}$$

Substituting eq. (10) into eq. (11) yields:

$$R_{x_1x_2}(\tau) = \alpha R_{ss}(\tau - D) + \alpha R_{sn_1}(\tau - D) + R_{sn_2}(\tau) + R_{n_1n_2}(\tau) \tag{12}$$

Assuming that the sound source signal $s(t)$ is uncorrelated with the noise signal, and the noise signals $n_1(t)$ and $n_2(t)$ are uncorrelated with each other, the cross-correlation function of $x_1(t)$ and $x_2(t)$ can be transformed into:

$$R_{x_1x_2}(\tau) = \alpha R_{ss}(\tau - D) \tag{13}$$

According to correlation function and autocorrelation principles, the cross-correlation function reaches its peak whenτ =D. The time τ corresponding to this peak is taken as the theoretical acoustic wave transit time. Figure 1 shows the correlation function, where the peak indicates the cross-correlation coefficient, and its position represents the acoustic wave transit time. The coefficient reflects the time delay between signals received by the two sensors. A cross-correlation coefficient approaching 1suggests high signal similarity, strong correlation, and low interference.

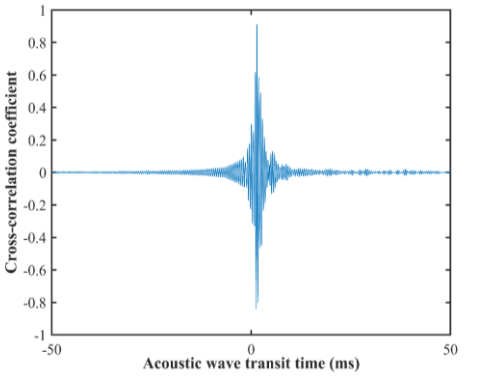

Fig. 1. Cross-correlation function

4.Experimental research

4.1.Coal sample preparation

The anthracite coal was selected as the research object for the experiment, and four particle sizes (0.6-0.8 cm, 0.8-1.2 cm, 1.2-3 cm, and 3-5 cm) were screened by crushing. Each component of the anthracite coal was precisely proportioned, thoroughly mixed, and loaded into the coal box following the proportion requirements listed in tab. 1.

Tab. 1. Coal sample particle size mixing ratio

Particle size	0.6-0.8 cm	0.8-1.2 cm	1.2-3 cm	3-5 cm
Proportion	10%	15%	55%	20%

4.2 Experimental setup and procedure

The experimental system includes a coal box, an acoustic test setup, and a temperature control system, as shown in fig.2 and fig.3. The coal box measures 100 cm × 30 cm × 30 cm. The acoustic system consists of a full-range loudspeaker, UPU40 sensor, UPU803 signal conditioner, A3001 power amplifier, and USB3133A data acquisition card. The temperature control system comprises asbestos insulation, a silicone heating plate, a K-type thermocouple, and a TA612C thermometer.

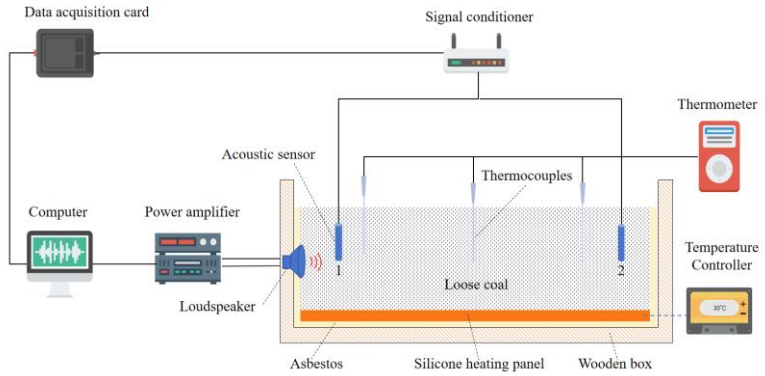

Fig. 2. Acoustic temperature measurement system for loose coal

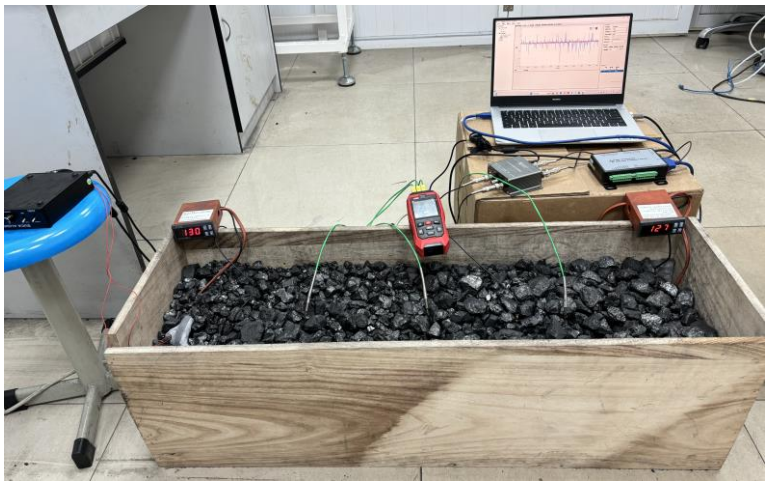

Fig. 3. Physical drawing of acoustic temperature measurement device

A mesh screen separates the loudspeaker from the loose coal, preventing interference with the speaker's diaphragm vibration. The acoustic sensor (UPU 40) has a frequency response range of 20 Hz to 20 kHz and a sensitivity of 26±1.5dB. The sensor was buried at a depth consistent with the center of the sound source, and the acoustic sensor 1 was fixed 5 cm directly in front of the sound source. The data acquisition card converted the acquired acoustic signal into a voltage signal with a sampling frequency of 500 kHz. K-type thermocouples were used to measure the temperature inside a loose coal body as a reference temperature. Three K-type thermocouples were buried equidistant from each other in the loose coal at a height consistent with the center of the sound source. The 10-mm-thick asbestos layer was installed at the bottom and sidewalls of the coal box for thermal insulation.

The computer-generated acoustic signal was amplified by a power amplifier and emitted through a loudspeaker. Sensors 1 and 2 received the signal and transmitted it to a signal conditioner. The acoustic signal was optimized by a signal conditioner and then converted to an electrical signal by a data

acquisition card, and transmitted to a computer for data processing.

To improve the accuracy of acoustic transit time measurements, a band-pass filter based on the Butterworth principle was applied to effectively suppress environmental noise. Zero-padding was used to reduce signal distortion caused by filter edge effects. A linear chirp signal (the spectrogram of the ideal linear swept signal is showed in fig. 4) was selected as the acoustic source to suppress sidelobes in the cross-correlation results and enhance the precision and stability of transit time estimation. The sampling frequency was set to 50,000 Hz. Each frequency was tested five times, and the average transit time was calculated using the cross-correlation method to ensure result reliability.

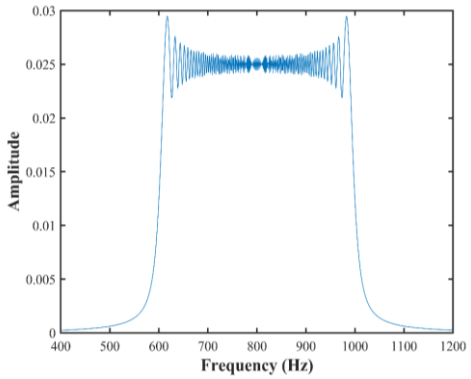

Fig. 4. Spectrogram of the ideal linear swept signal

4.2.Results and analysis

4.2.1. Acoustic wave transit time at different frequencies

The sensor spacing under 20 °C conditions was set at 0.6 m. Figure 5 shows the acoustic transit times for 14 frequency sets ranging from 200 to 3000 Hz at 200 Hz intervals.

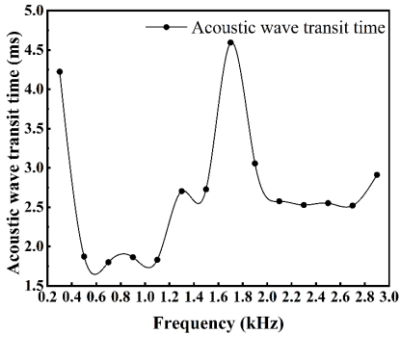

Fig. 5. Acoustic wave transit time at different frequencies

The acoustic wave transit time showed a fluctuating trend with increasing frequency. When the acoustic signal frequency ranges from 200-400 Hz and 1600-1800 Hz, the acoustic wave transit time exhibited significant peak variations and reached its maximum value at 1600-1800 Hz, indicating that the acoustic wave was significantly affected at this frequency. The transit time of acoustic waves was shorter, the fluctuation amplitude was less, and the change trend was more stable at low frequencies (400-1000 Hz) and high frequencies (2000-3000 Hz). This effect likely results from the fact that in the low-frequency sound wave range, acoustic wave propagation is less affected by interference or reflection due to the longer wavelength of the waves. The shorter wavelengths of high-frequency sound waves

may cause the averaging of multiple interference effects, reducing the overall fluctuation amplitude.

The complex pore structure of coal tends to cause significant scattering, reflection, or local resonance of acoustic waves in specific frequency bands. According to Biot's theory of acoustic propagation in porous media[27], sound waves can propagate in dual modes through both the solid frame and the pore gas within the solid-gas coupled system. Energy coupling and viscous dissipation between these paths are key factors contributing to the notable fluctuations in time-of-flight at certain frequencies. In the low-frequency range (400-1000 Hz), the wavelength is much larger than the typical pore size, leading to weak scattering and stable propagation. In the high-frequency range (2000-3000 Hz), although the wavelength is shorter, the signal remains strong over short distances and can penetrate some micropores, showing resistance to scattering. Using these bands in acoustic thermometry can enhance data reliability and consistency while reducing measurement errors. Future studies will incorporate techniques such as CT scanning and mercury intrusion porosimetry to obtain pore structure data. The relationship between wavelength and structural scale will be further examined to develop a frequency optimization model based on pore characteristics.

4.2.2. Acoustic wave transit time at different sensor spacings

To further explore the acoustic properties of loose coal, five frequency ranges (400-1000 Hz, 500-1200 Hz, 600-1400 Hz, 700-1600 Hz, and 2000-3000 Hz) were selected for subsequent experiments based on the above analysis results. This selection aims to minimize the impact of overly narrow or wide frequency bands on the experiment. At 20 °C, the spacing between two sensors was set to 0.15 m, 0.3 m, 0.45 m, 0.6 m, and 0.75 m. To get the average value, 25 groups of working circumstances were evaluated; each group was tested five times.

Figure 6 shows the acoustic wave transit time at different sensor spacings. The acoustic wave transit time increased with sensor spacing, but the rate of increase varied across frequency ranges. In the 400-1000 Hz and 2000-3000 Hz bands, transit time showed a consistent upward trend. In stacked loose coal, wave propagation is affected by attenuation factors such as absorption, scattering, and multipath effects. The 400-1000 Hz range experienced less attenuation, resulting in a steadier increase in transit time with distance. In the 2000-3000 Hz range, high-frequency waves were less affected by particle interactions at short distances, leading to stable propagation velocity due to strong signals and limited scattering.

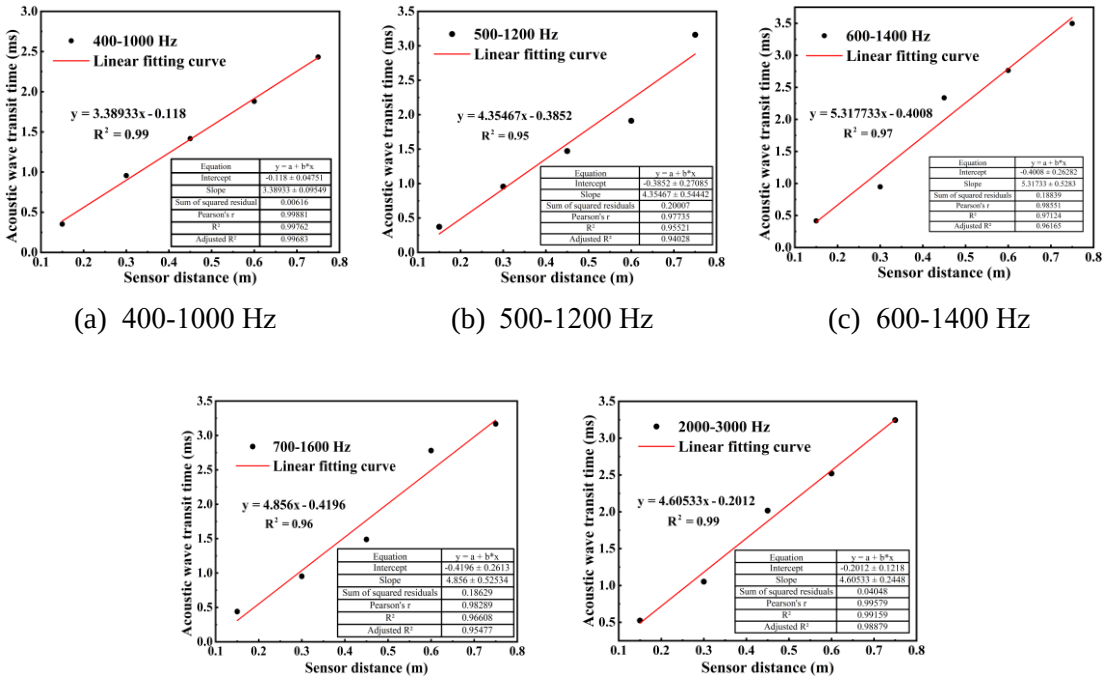

(a) 400-1000 Hz (b) 500-1200 Hz (c) 600-1400 Hz

(d) 700-1600 Hz (e) 2000-3000 Hz

Fig. 6. Acoustic wave transit time at different sensor spacings

Acoustic wave propagation in loose coal accumulations shows a strong path effect. As the sensor spacing increases, signal attenuation becomes more significant. In high-frequency bands, the signal may drop below the noise threshold, reducing cross-correlation peak clarity and lowering the signal-to-noise ratio. Meanwhile, the heterogeneous structure of the coal body enhances multipath scattering over longer paths, which increases transit time errors. Therefore, long-distance measurements require a balance between signal quality and measurement accuracy. Proper spacing, combined with filtering and signal enhancement, is essential to ensure inversion reliability.

4.2.3. Acoustic wave transit time at different temperatures

To investigate the applicability of acoustic thermometry in the initial heating stage of loose coal, this experiment comprehensively considered the influence of acoustic frequency and sensor spacing on propagation characteristics. Three frequency bands (400-1000 Hz, 600-1400 Hz, and 2000-3000 Hz) were selected, combined with three spacing distances (0.45 m, 0.6 m, and 0.75 m). Heating experiments were conducted within the range of 20-50 °C [17, 21] to measure the characteristics of acoustic transit time under different conditions, laying a foundation for the subsequent extension of the model to higher temperature stages.

Figure 7 shows the variation of acoustic wave transit time with temperature at three frequencies. At three different frequencies and sensor spacing conditions, transit time decreased as temperature increased. Higher temperatures increase gas molecule activity in pores, raising acoustic velocity and reducing transit time. At 0.6 m and 0.75 m spacings, high-frequency waves showed a larger decrease in transit time than low and mid frequencies, indicating greater sensitivity to changes in coal structure, porosity, and gas density. During heating, the solid skeleton of coal, composed of organic matter and minerals, undergoes slight thermal expansion. This compresses the pore structure and reduces porosity

[28]. Lower porosity increases the solid fraction per unit volume and may change the coal's density. As a result, the contribution of the solid frame to wave propagation becomes more significant. The overall behavior tends to follow the "fast wave" mode in Biot's theory, leading to higher sound velocity and a decrease in the acoustic wave transit time.

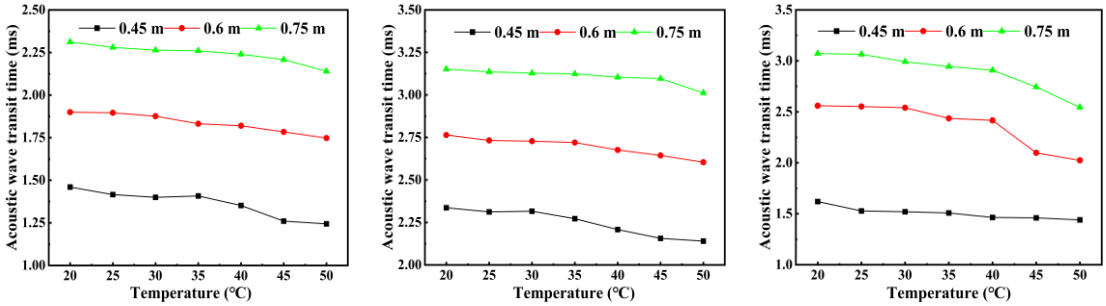

(a) 400-1000 Hz (b) 600-1400 Hz (c) 2000-3000 Hz

Fig. 7. Variation of acoustic wave transit time with temperature at three frequencies

The acoustic thermometry system was used to measure the acoustic wave transit time through two distinct media: loose coal (t) and air (t_0). The characterization factor$\lambda$was calculated according to the formula. The calculation results are shown in the tab. 2.

Tab. 2. Calibration of the characteristic factors

Sensor distance/ m	Acoustic frequency/ Hz	t / ms	t_0/ ms	Calculation formula	λ
0.45	400-1000	1.46	1.312		1.115
0.45	600-1400	2.336	1.3		1.783
0.45	2000-3000	1.62	1.32		1.237
0.6	400-1000	1.9	1.76		1.086
0.6	600-1400	2.764	1.78	$\lambda = \frac{t}{t_0}$	1.579
0.6	2000-3000	2.56	1.772		1.463
0.75	400-1000	2.312	2.22		1.061
0.75	600-1400	3.152	2.2		1.446
0.75	2000-3000	3.072	2.18		1.408

Combined with the calculated values of the characterization factor obtained from tab. 2, the acoustic temperature measurement model was used to invert the temperature, the inversion results are shown in fig. 8. The relative error was calculated to be in the range of 2.27%-7.13% based on the inversion temperature versus the reference temperature measured by the thermocouple. The results show that the measured acoustic wave transit time has a good mapping relationship with the temperature. Additionally, the constructed acoustic wave transit time-coal temperature model exhibits high accuracy and reliability, enabling effective temperature inversion. Compared with traditional temperature measurement methods such as infrared and distributed optical fiber sensing, acoustic thermometry offers advantages including non-contact operation, flexible deployment, and wide adaptability. However, it is more susceptible to environmental noise and requires filtering and signal enhancement techniques to

ensure measurement stability.

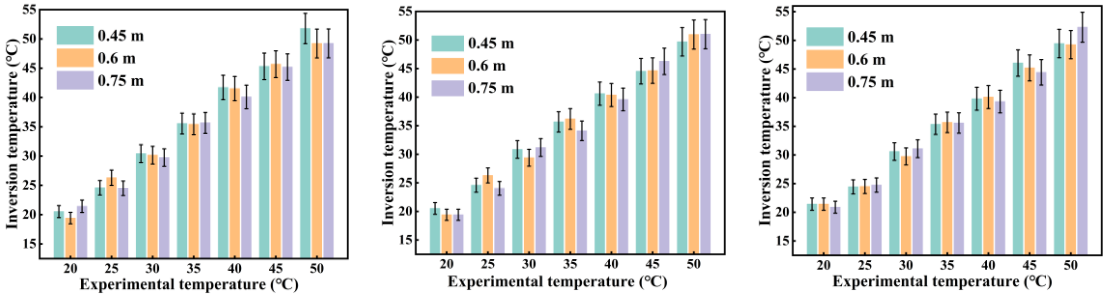

(a) 400-1000 Hz (b) 600-1400 Hz (c) 2000-3000 Hz

Fig. 8. Acoustic thermometry model inversion temperature results

In order to analyze the sources of inversion error, this study considers three aspects: instrument performance, model assumptions, and environmental factors. On the instrument side, the ±1.5 dB sensitivity deviation of the sensors and the 25 kHz sampling rate limit waveform identification and time resolution. In terms of the model, a characteristic factor$\lambda$was introduced to correct sound velocity under varying frequencies and distances. Although it achieved good overall fitting, its performance is limited under complex structures and nonlinear thermal responses. Environmentally, uncontrolled coal moisture may affect acoustic properties. To suppress external noise, a Butterworth-based bandpass filter was designed with optimized cutoff frequencies. Zero-padding was also applied to reduce edge distortion from filtering. After these measures, the inversion results showed good stability and repeatability.

To further improve the adaptability and accuracy of the model, coal samples with different porosity and particle size distributions will be introduced. Techniques such as CT scanning and mercury intrusion porosimetry will be used to develop a statistical model linking λ to structural parameters. This will help optimize the correction mechanism. In parallel, controlled humidity experiments are planned to quantify the effect of moisture changes on acoustic wave propagation and temperature inversion accuracy. To extend the model's applicability to higher temperatures, a stepwise heating experiment from 50 °C to 120 °C will be conducted. By analyzing the dynamic relationship between coal pyrolysis characteristics and acoustic parameters, a nonlinear extrapolation model of temperature-velocity response will be established. These efforts aim to provide theoretical support for the application of acoustic thermometry and full-cycle spontaneous combustion monitoring.

5.Conclusions

This study developed a temperature measurement system for loose anthracite coal. Acoustic transit times were measured under varying frequencies, sensor spacings, and temperatures. Based on the results, the effects of frequency, spacing, and temperature on transit time were systematically analyzed. The main conclusions are as follows:

(1) At acoustic frequencies of 200-400 Hz and 1600-1800 Hz, the acoustic transit time exhibits significant peak variations. In contrast, the 400-1000 Hz and 2000-3000 Hz bands show minimal transit time fluctuation, stable trends, and superior wave propagation, making them more suitable as preferred ranges for acoustic transit time testing.

(2) The acoustic wave transit time increases with distance for different sensor spacing conditions. When the acoustic wave range is between 400-1000 Hz and 2000-3000 Hz, the acoustic wave transit

time tends to increase steadily with the sensor spacing. This indicates that in these frequency ranges, the velocity of sound wave propagation is relatively stable and suitable for acoustic measurements.

(3) The acoustic wave transit time showed an overall decreasing trend with increasing temperature. The model based on the mapping relationship between acoustic wave transit time and temperature can well invert the coal temperature, and its relative error is 2.27%-7.13%, which verifies the reliability and accuracy of the model. Stable transit time extraction was achieved at sensor spacings of 0.45-0.75 m. After signal processing, a good signal-to-noise ratio was obtained under laboratory conditions. For future field applications, increasing excitation intensity and optimizing frequency matching are recommended to adapt to complex noise environments.

Acknowledgment

This work was supported by the Zhejiang Provincial Natural Science Foundation of China [Grant No. LY18E040001].

Nomenclature

c - velocity of sound waves, [ms^{-1}]
P - gas pressure, [pa]
ρ -gas density, [kgm^{-3}]
V - volume of ideal gas, [m^3]
M - gas mas, [kg]
R - gas constant, [JK^{-1}mol^{-1}].
Z - velocity of sound constant
T - temperature, [℃]
l - the propagation distance, [m]
t - acoustic wave transit time, [s]
$x(t)$ - acoustic signal
$s(t)$ - sound source signal
$n(t)$ - the noise of the signal
D - actual acoustic wave transit time, [s]
R - cross-correlation function

Greek symbols

γ - specific heat capacity ratio
μ - molar amount of gas, [kgmol^{-1}]
λ - characterization factor
α - attenuation coefficient

References

[1] Jingxin, S., *et al.*, Case study on wastewater treatment technology of coal chemical industry in China, *Critical Reviews in Environmental Science and Technology*, *51*. (2020), 10, pp. 1-42, DOI No. 10.1080/10643389.2020.1742530
[2] Jia, Z.,B. Lin, How to achieve the first step of the carbon-neutrality 2060 target in China: The coal substitution perspective, *Energy*, *233*. (2021), DOI No. 10.1016/j.energy.2021.121179
[3] Li, X.-R., *et al.*, A STUDY ON SPONTANEOUS IGNITION OF BITUMINOUS COAL, *Thermal Science*, *13*. (2009), 1, pp. 105-112, DOI No. 10.2298/tsci09011051
[4] Liang, X., *et al.*, STUDY OF FRACTAL BASED OXYGEN ADSORPTION EXPERIMENT OF POROUS COAL, *Thermal Science*, *26*. (2022), 1, pp. 517-527, DOI No. 10.2298/tsci2010080621
[5] Bing-Rui, Y., *et al.*, A novel intumescent flame-retardant to inhibit the spontaneous combustion of coal, *Fuel*, *297*. (2021), DOI No. 10.1016/j.fuel.2021.120768
[6] Zhang, Y., *et al.*, Characteristics of mass, heat and gaseous products during coal spontaneous combustion using TG/DSC–FTIR technology, *Journal of Thermal Analysis and Calorimetry*, *131*. (2018), 3, pp. 2963-2974, DOI No. 10.1007/s10973-017-6738-x
[7] John, M., *et al.*, Ultrasonic measurement of temperature distributions in extreme environments: Electrical power plants testing in utility-scale steam generators, *Ultrasonics*, *138*. (2024), DOI No. 10.1016/j.ultras.2023.107205
[8] Guo, G., *et al.*, Measurement of 2-D Temperature Distribution in a Biomass Silo Through

Acoustic Tomography, *Ieee Transactions on Instrumentation and Measurement*, *74*. (2025), DOI No. 10.1109/tim.2025.3541755
[9] Huang, H., *et al.*, Short-Range Water Temperature Profiling in a Lake with Coastal Acoustic Tomography, *Sensors*, *20*. (2020), 16, DOI No. 10.3390/s20164498
[10] Yan, H., *et al.*, *Research on Estimation of Acoustic Travel-time in Soybeans*, *International Conference on Measuring Technology and Mechatronics Automation*. 2009: Zhangjiajie, PEOPLES R CHINA. p. 832-835.
[11] Rindel, J.H., Air Attenuation in Octave Bands and How to Normalize Room Acoustic Measurements to a Standard Atmosphere, *Applied Sciences-Basel*, *14*. (2024), 22, DOI No. 10.3390/app142210139
[12] Kong, Q., *et al.*, Acoustic tomography method for temperature and velocity fields simultaneous measurement, *Measurement*, *250*. (2025), DOI No. 10.1016/j.measurement.2025.117198
[13] Yan, Y., *et al.*, Passive acoustic measurements of air temperature at various altitudes, *The Journal of the Acoustical Society of America*, *157*. (2025), 2, pp. 1290-1301, DOI No. 10.1121/10.0035794
[14] Huang, H., *et al.*, Continuously sensing of water temperature in a lake using acoustic tomography method, *Remote Sensing Letters*, *13*. (2022), 3, pp. 219-225, DOI No. 10.1080/2150704X.2021.2017506
[15] Yan, H., *et al. Measurement of Acoustic Wave Travel-Time in Grain Bulk*,28th Chinese Control and Decision Conference,Yinchuan, PEOPLES R CHINA,2016, pp. 1137-1142
[16] Yan, H., *et al.*, Primary study of temperature distribution measurement in stored grain based on acoustic tomography, *Experimental Thermal and Fluid Science*, *42*. (2012), pp. 55-63, DOI No. 10.1016/j.expthermflusci.2012.04.010
[17] Guo, J., *et al.*, Exploring Acoustic Wave Propagation and Equivalent Path in Quasi-Porous Medium of Loose Coal Mass, *Natural Resources Research*, *33*. (2024), 1, pp. 389-403, DOI No. 10.1007/s11053-023-10297-y
[18] Guo, J., *et al.*, Early Detection of Coal Spontaneous Combustion by Complex Acoustic Waves in a Concealed Fire Source, *Acs Omega*, *8*. (2023), 19, pp. 16519-16531, DOI No. 10.1021/acsomega.3c00199
[19] Liu, Y., *et al.*, Time Delay Estimation for Acoustic Temperature Measurement of Loose Coal Based on Quadratic Correlation PHAT-β Algorithm, *Fire*, *7*. (2024), 7, pp. 228-228, DOI No. 10.3390/fire7070228
[20] Wang, J., *et al.*, Acoustic wave propagation characteristics and spontaneous combustion warning of coal during oxidative warming of loose coal, *Fuel*, *398*. (2025), DOI No. 10.1016/j.fuel.2025.135528
[21] Deng, J., *et al.*, Investigation on high temperature point detection of spontaneous combustion of loose coal based on optimal acoustic signal, *Process Safety and Environmental Protection*, *185*. (2024), pp. 423-434, DOI No. 10.1016/j.psep.2024.03.028
[22] Kong, B., *et al.*, Study on sound wave kinematic characteristics and temperature sensing mechanism during the warming process of loose coals, *Energy*, *307*. (2024), DOI No. 10.1016/j.energy.2024.132753
[23] Wilk, G.,Z. Wlodarczyk, Temperature oscillations and sound waves in hadronic matter, *Physica a-Statistical Mechanics and Its Applications*, *486*. (2017), pp. 579-586, DOI No. 10.1016/j.physa.2017.06.006
[24] Guo, H., *et al.*, Numerical simulation of adsorption process of O_2/H_2O mixed gas in coal porous media, *International Journal of Coal Science & Technology*, *11*. (2024), 1, DOI No. 10.1007/s40789-024-00714-9
[25] Yoo, J.-C.,T.H. Han, Fast Normalized Cross-Correlation, *Circuits Systems and Signal Processing*, *28*. (2009), 6, pp. 819-843, DOI No. 10.1007/s00034-009-9130-7
[26] Karlovic, I., *et al.*, Analysis of the hydraulic connection of the Plitvica stream and the groundwater of the Varazdin alluvial aquifer, *Geofizika*, *38*. (2021), 1, pp. 15-35, DOI No. 10.15233/gfz.2021.38.3
[27] Biot, M.A., Theory of Propagation of Elastic Waves in a Fluid‐Saturated Porous Solid. II. Higher Frequency Range, *The Journal of the Acoustical Society of America*, *28*. (1956), 2, pp. 179-191, DOI No. 10.1121/1.1908241
[28] Su, X.Y., *et al.*, Thermal Expansion and Adsorption Characteristics of Coal Based on Temperature Change and Its Influence on the Slippage Effect, *Energy & Fuels*, *37*. (2023), 9, pp. 6558-6568, DOI No. 10.1021/acs.energyfuels.3c00513

Received: 29.4.2025.
Revised: 26.7.2025.
Accepted: 5.9.2025